DOI: 10.19884/j.1672-5220.202312005

Impact Behavior Analysis and Failure Mode Comparison of Glass Fiber (GF)/Polydicyclopentadiene (PDCPD) Thermosetting Composite for Automobile Bottom Protection Plate

MEI Zhonghao[1], PEI Zhilei[1], CHENG Lele[1], MIN Wei[1], GAO Ruize[1], CHENG Chao[1,2], ZHOU Fei[3], YU Muhuo[1], SUN Zeyu[1*]

1. College of Materials Science and Engineering, Shanghai Key Laboratory of Lightweight Structural Composites, Shanghai Collaborative Innovation Center of High-Performance Fibers and Composites, Donghua University, Shanghai 201620, China
2. Shanghai Carbon Fiber Composites Innovation Institute Co., Ltd., Shanghai 201512, China
3. Sinopec Shanghai Petrochemical Co., Ltd., Shanghai 200540, China

Abstract: A glass fiber (GF)/polydicyclopentadiene (PDCPD) composite impact simulation model was established based on LS-DYNA (the finite element analysis software peroduced by Livermore Software Technology Corporation) simulation. An optimal ply thickness of the composite GF/PDCPD was determined as 3.0 mm, and thus the final intrusion depth was controlled within 8.8 mm, meeting the performance standards for battery electric vehicle protection materials. A comparative analysis of failure modes during impacts was conducted for composites GF/PDCPD, GF/polypropylene (PP) and GF/polyamide (PA). The results indicated that GF/PDCPD exhibited compressive failure modes and ductile fractures, resulting in smaller damage areas. In contrast, GF/PP and GF/PA showed fiber fracture failures, leading to larger damage areas. The molding process and impact resistance of GF/PDCPD were investigated. By comparing the impact performance of GF/PDCPD with that of GF/PP and GF/PA, it was concluded that GF/PDCPD demonstrated superior performance and better alignment with the performance standards of battery electric vehicle protective materials. The predictability and accuracy of LS-DYNA simulation was verified, providing a theoretical foundation for further in-depth research.

Key words: thermosetting composite; PDCPD; GF/PP; GF/PA; LS-DYNA simulation; impact performance; MAT54

CLC number: TB332 **Document code**: A

Article ID: 1672-5220(2024)06-0595-12

Open Science Identity (OSID)

0 Introduction

Currently, composite materials have emerged as a key focus area in the development of battery protective plate materials for electric vehicles. The necessity to create a battery underbody shield that can effectively safeguard the battery from impacts is paramount. These underbody guards need to provide robust protection against collisions while maintaining minimal deformation and lightweight construction to enhance the fuel efficiency of electric vehicles[1-2]. As such, the utilization of lightweight composites is essential for reducing vehicle weight[2-6], and cost-effective materials must be chosen for future industrial applications. In order to satisfy these requirements, the adoption of glass fiber reinforced polymer (GFRP) composites known for their exceptional toughness and impact resistance, represents an optimal solution for underbody protection.

However, traditional thermosetting resin composites face significant limitations in the industrial sector due to slow manufacturing, high cost and low recyclability. Polydicyclopentadiene (PDCPD), a novel thermosetting resin produced through organometallic catalyzed ring-opening translocation polymerization of monomeric dicyclopentadiene (DCPD), offers a promising solution due to its unique combination of toughness and rigidity[6-8]. Due to its low monomer viscosity, once the reaction is triggered by the addition of a catalyst, the polymerization completes in a very short time. A variety of parts used in automotive shells and other large-scale engineering applications have been prepared by reaction injection molding (RIM), and its industrial development has become increasingly mature[9]. PDCPD has low monomer viscosity, enabling rapid polymerization upon the addition of a catalyst, and thus is suitable for use in RIM for large-scale engineering applications. Furthermore, thermoplastics such as polyethylene terephthalate can be used as matrices due to their cost-

Received date: 2023-12-16

* Correspondence should be addressed to SUN Zeyu, email: sunzeyu@dhu.edu.cn

Citation: MEI Z H, PEI Z L, CHENG L L, et al. Impact behavior analysis and failure mode comparison of glass fiber (GF)/polydicyclopentadiene (PDCPD) thermosetting composite for automobile bottom protection plate[J]. *Journal of Donghua University (English Edition)*, 2024, 41(6): 595-606.

effectiveness, formability and recyclability[10-11]. In comparison to epoxy resins, they are often more viscous and challenging to process[8,12]. PDCPD composites have demonstrated excellent impact resistance in multiple studies[13-14]. Vallons et al.[13] obtained glass fiber (GF)/PDCPD composites by vacuum-assisted molding. The results show that PDCPD composites exhibit excellent impact resistance compared with epoxy composites. Hu et al.[14] studied the effect of damp heat aging on the tensile fatigue behavior of unidirectional GF/PDCPD composites, which exhibited less water absorption and better fatigue properties than similarly aged epoxy composites. This is attributed to the inherent hydrophobicity of PDCPD resins. The combination of PDCPD and GF presents an affordable and effective solution for various applications, particularly in lightweight and high-strength structures.

In this study, linear polymerization of DCPD monomer without cross-linking was conducted by adjusting the catalyst content to achieve the desired viscosity for the resin obtained by vacuum assisted resin infusion (VARI). GFs were treated and combined with PDCPD to create GF/PDCPD laminates. Among the thermoplastic polymers of GFRP composites, polypropylene (PP) and polyamide (PA) are widely used in the industrial field and have the advantage of particularly excellent shock absorption[11,15]. So GF/PP and GF/PA laminates were prepared for comparison. Mechanical tests were performed on these laminates to evaluate their tensile, compression and shear properties, laying the groundwork for material card parameters in simulation models.

The study of low-speed impact is valuable in analyzing various impact events, and understanding the behavior of composite structures under low-speed impact is crucial for enhancing the impact resistance of composite materials. Experimental test methods can be employed to investigate the low-speed impact behavior of composite materials. Numerical simulation methods offer the advantage of damage prediction and can provide a better understanding and prediction of this behavior. Therefore, a combination of experimental tests and simulations is often preferred for studying the low-speed impact behavior of composite materials.

GF reinforced composites exhibit relatively good performance under low-speed impact, whereas carbon fiber reinforced composites display relatively poor performance under the same conditions[16]. Moreover, specific studies have been conducted on the mechanical response of GF/PP composites under low-speed impact, demonstrating that the composite performance can be enhanced by adjusting the GF content and the number of layers[17]. As a result of these adjustments, the composites exhibit improved low-speed impact performance. This research underscores the potential for optimizing composite materials through careful adjustments to their composition and structure, thereby enhancing their suitability for various applications. Kumar et al.[18] explored the potential to minimize damage from low-velocity impacts in composite foam core sandwich structures by enhancing their perforation resistance. This was achieved by integrating a reinforced impregnated paper honeycomb (RIPH) structure into the composite foam during the manufacturing process. The results indicate that the peak impact load-bearing capacity and damage tolerance of the sandwich composites are entirely dependent on the level of impact energy. The pore size of the foam core with the RIPH structure significantly affects the extent of impact damage and the energy absorption mechanisms in the sandwich composites. The improvement in the energy absorption characteristics and damage tolerance of the hardened composite foam core sandwich structures is attributed to the unit size of the RIPH structure. Um et al.[10] used ABAQUS (the finite element analysis software usually used for simulating physical processes in engineering) to simulate the crash of the underbody skid plate. By analyzing the simulated failure process of the underbody skid plate of different thicknesses, it was determined that the shield with the best impact resistance was 2.4 mm thick, weighed 3.88 kg and was 52% lighter than the steel material.

Among existing software, LS-DYNA is widely used in the literature to simulate low-speed impact events. It provides an extensive library of composite material models and contact algorithms, including cohesive material models. In particular, Material Type 54 (MAT54) provides favorable parameters. Heimbs et al.[19] used MAT54 to simulate low-speed impact events of preloaded CFRPs. They obtained very precise results in terms of force-time and energy-time curves. Ge et al.[20] tested several material models using the user-defined material subprogram (VUMAT) in ABAQUS for the specifics of low-speed impact unidirectional CFRPs. The main conclusion they reached was that the Puck criterion[21] was the most adequate. This criterion considers an inclined fracture surface for matrix compression. However, such material models require very specific experimental parameters and are difficult to obtain. Therefore, experimental tests are needed to obtain experimental data to establish material cards to help build simulation models[22-26].

In our previous work, the best prepolymer formulation of PDCPD suitable for the low-cost composite moulding process (e.g. VARI) was selected experimentally[28]. In this study, GF is utilized as the reinforcement, while PDCPD, PP and PA are used as the matrix resins to create composites with high impact resistance. The basic parameters of the MAT54 material card through the experiments are obtained. Specifically, we conducted quasistatic uniaxial tensile, compression and in-plane shear tests on GF/PDCPD, GF/PP and GF/PA to obtain their fundamental strength parameters, such as tensile strength (XT/YT), tensile modulus (EA/

EB), compressive strength (XC/YC), in-plane shear strength (SC) and in-plane shear modulus (GAB). The results provide important data for understanding the behavior of the composite materials and optimizing their compositions and structures to enhance their performance in various applications[28], and a complete material card is established. LS-DYNA is used to construct a laminate impact simulation model[29-31]. The impact behavior and failure modes of the laminate under impact loading are thoroughly investigated, leading to the development of an impact-resistant laminate with optimized ply thickness. A comparative analysis of the impact failure modes for GF/PDCPD, GF/PA and GF/PP composites is conducted, focusing on impact strength and failure characteristics. The error analysis is also performed using simulation models to validate the consistency between the actual failure modes, mechanical responses and the trends predicted by the simulations. By integrating experimental data and simulation results, a practical and predictive "new material" composite laminate impact performance simulation system is established. This system enables researchers and engineers to assess the impact resistance of composite materials accurately, predict failure modes, and optimize design parameters for enhanced performance and durability in real-world impact scenarios.

In this paper, the impact behavior and failure modes of composite materials are examined with a particular focus on GF/PDCPD thermosetting composites used in automobile underbody protection plates. The optimal ply thickness of these composites is explored, and their impact resistance and failure characteristics are compared with those of traditional thermoplastic composites GF/PP and GF/PA. By integrating experimental testing with numerical simulations, the research aims to improve the impact resistance and damage tolerance of automotive protective materials, advancing the development of lightweight and high-performance vehicle components.

1 Materials and Methods

1.1 Materials and sample preparation

DCPD was obtained from Shanghai Petrochemical Co., Ltd., China. Grubbs second-generation catalyst (GC2), tributyl phosphite (TBP), cyclohexylbenzene (CHB) and ethyl norbornene (ENB) were obtained from Shanghai Aladdin Biochemical Technology Co., Ltd., China. GF, PP and PA were obtained from Shanghai HAMM Construction Technology Co., Ltd., China. Polystyrene (PS) was obtained from Shanghai SECCO Petrochemical Co., Ltd., China. Polystyrene-polybutadiene-polystyrene copolymer (SBS) was obtained from Baling Petrochemical Co., Ltd., China. The PA6 thermoplastic resin and the PP thermoplastic resin were obtained from Hummer Construction Technology Co., Ltd., China.

The viscosity of the resin used for VARI is usually limited to 100–500 mPa·s with good stability, where the liquid monomer needs to last at least 5 h. Through experimental comparison and verification, the PDCPD resin suitable for the VARI molding process was obtained. The mass ratio of DCPD monomer to GC2 is $1:3\times10^{-5}$, and its viscosity can reach 300–400 mPa·s at 25 ℃ to meet the experimental requirements. The PDCPD resin curing process parameters are shown in Table 1.

Table 1 Curing process parameters for PDCPD resin

Stage	Temperature/℃	Hold time/h
Stage Ⅰ	45	0.5
Stage Ⅱ	60	0.5
Stage Ⅲ	120	1.0

Preparation of GF/PDCPD composites by the VARI molding process is shown in Fig. 1. Tempered glass (a thickness of 10 mm) was used as the mold, cleaned with acetone and coated with a mold release agent. The mold release cloth and guide net are put in the middle of the mold when the fabric is placed. It is crucial to align the fabric both vertically and horizontally. Ensuring the flatness of all materials is important to prevent wrinkles during the vacuum process, as the wrinkles can cause defects in the laminate and weaken its mechanical properties. The sealing tape was applied around the area without the release agent. Two draft tubes were inserted in the corresponding positions: one to connect the vacuum pump and the other to fill the resin. To ensure that the vacuum bag fitted well on the fabric and the draft tubes without other forces, the vacuum was then engaged, and then the curing and demolding work was carried out.

First, the prepared specimens were cut by the composite computer numerical control cutting machine (Shanghai Huazi New Materials Technology Co., Ltd., China). The size of the specimen was in accordance with the relevant ASTM standards (ASTM D3039 for the tensile test, ASTM D6641 for the compression test, and ASTM D7078 for the in-plane shear test). Then the specimens were soaked in acetone at room temperature for 48 h, in ethanol for 1 h, and dried in an oven at 80 ℃. Finally, the specimens were sanded around the edges and then labeled.

The composite process flow diagram for GF/PP and GF/PA is shown in Fig. 2.

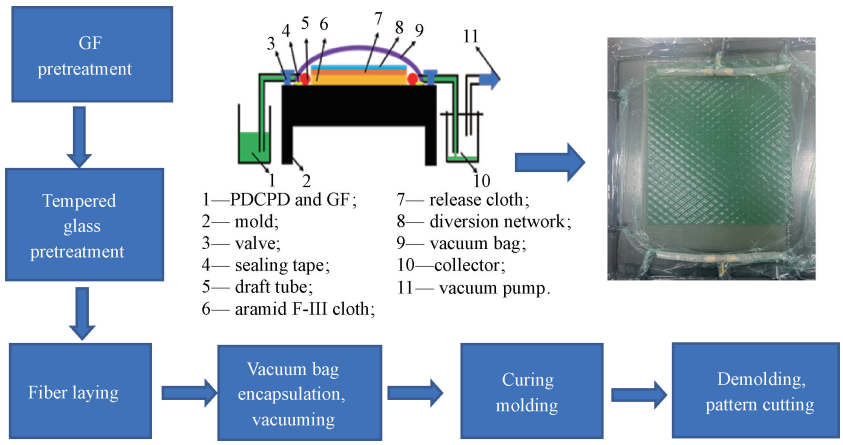

Fig. 1 VARI molding process flow diagram for GF/PDCPD

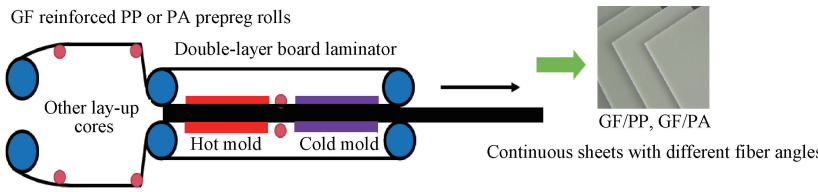

Fig. 2 Composite process flow diagram for GF/PP and GF/PA

The process of preparing GF/PP and GF/PA is as follows.

1) The upper and lower layers of the prepreg are put into the double-layer board laminator.

2) The material enters the hot mold and the cold mold in turn.

3) The material is impregnated in the hot mold and becomes a whole.

4) The whole material is cooled and shaped in the cold mold.

5) The continuous sheets with different fiber angles are obtained.

1.2 Test characterization

1.2.1 Establishment of the material card and simulation impact model

Through the test of tensile, bending and shear properties of GF/PDCPD, GF/PP and GF/PA composites, the basic test data and the basic material properties of the three composite laminates were obtained. The material card of the finite element simulation was established, and the three-dimentional (3D) effect diagram of the hammer impact laminate was drawn by the drawing software CATIA. The material card was then imported into the software HyperMesh for meshing, modling, etc. The SHELL163 shell elements were used to simulate the ply structure of composite laminates, mainly for the thickness of the ply. Additionally, the SOLID164 solid elements were employed to simulate hammerheads[26-27].

The impact simulation model is shown in Fig. 3. The laminates were divided using a quadrilateral grid with a length of 340 mm, a width of 240 mm, an element size of 2.0 mm × 2.0 mm and a quantity of 20 400 units. A hammer body was divided using high-quality hexahedral solid elements. To give the relevant materials and properties to the structural parts, the hammer body was modelled with a MAT-20 material card. The specific parameters are shown in Table 2. The impact process of the composite laminate was simulated using the material model MAT54 MAT_ENHANCED_COMPOSITE_DAMAGE of ANSYS/LS-DYNA.

First, the parameters for elastic material properties were input, including density, modulus of elasticity, Poisson's ratio and shear modulus. Next, the boundary conditions, load settings and contact settings of the model were established, where the contact settings were defined by the contact relationships, the response time and the punch speed. The output K file was simulated by LS-DYNA. Finally, the obtained d3plot file was imported into the postprocessing software LS-PrePost for analysis of simulation results.

As shown in Fig. 4, the mechanical property testing results of GF/PDCPD, GF/PP and GF/PA composites were obtained. Acetone depulping was carried out on the GF surface before the test and then compounded with PDCPD. The tensile, compression and in-plane shear properties of GF/PDCPD, GF/PP and GF/PA were tested, and the simulated material card parameters were obtained.

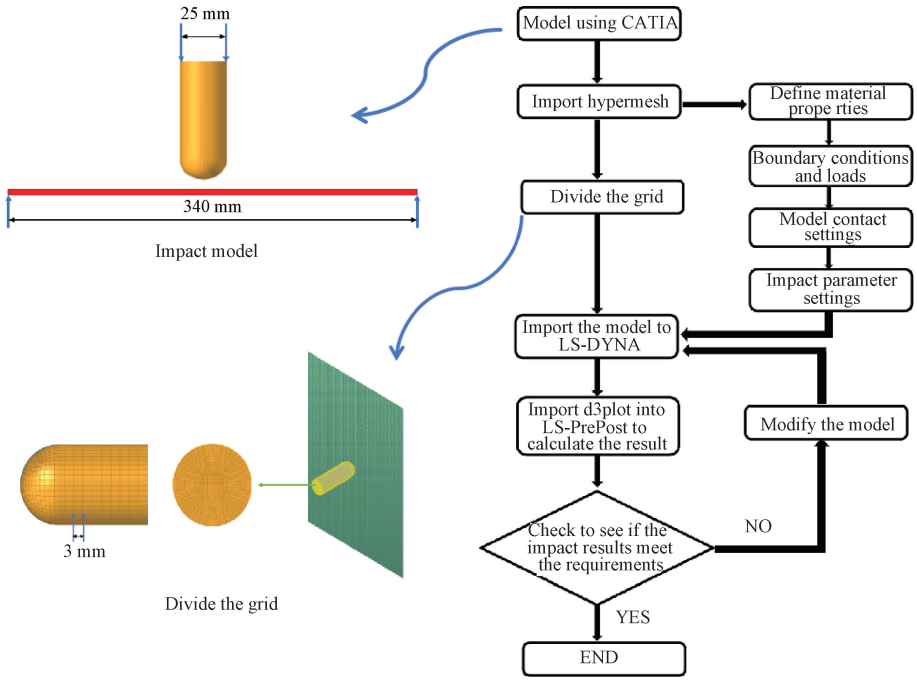

Fig. 3 Impact simulation model

Table 2 Punch material parameters

Material card	Density/(kg/mm^3)	Poisson's ratio	Elastic modulus/GPa
MAT-20	2.94×10^{-4}	0.3	210

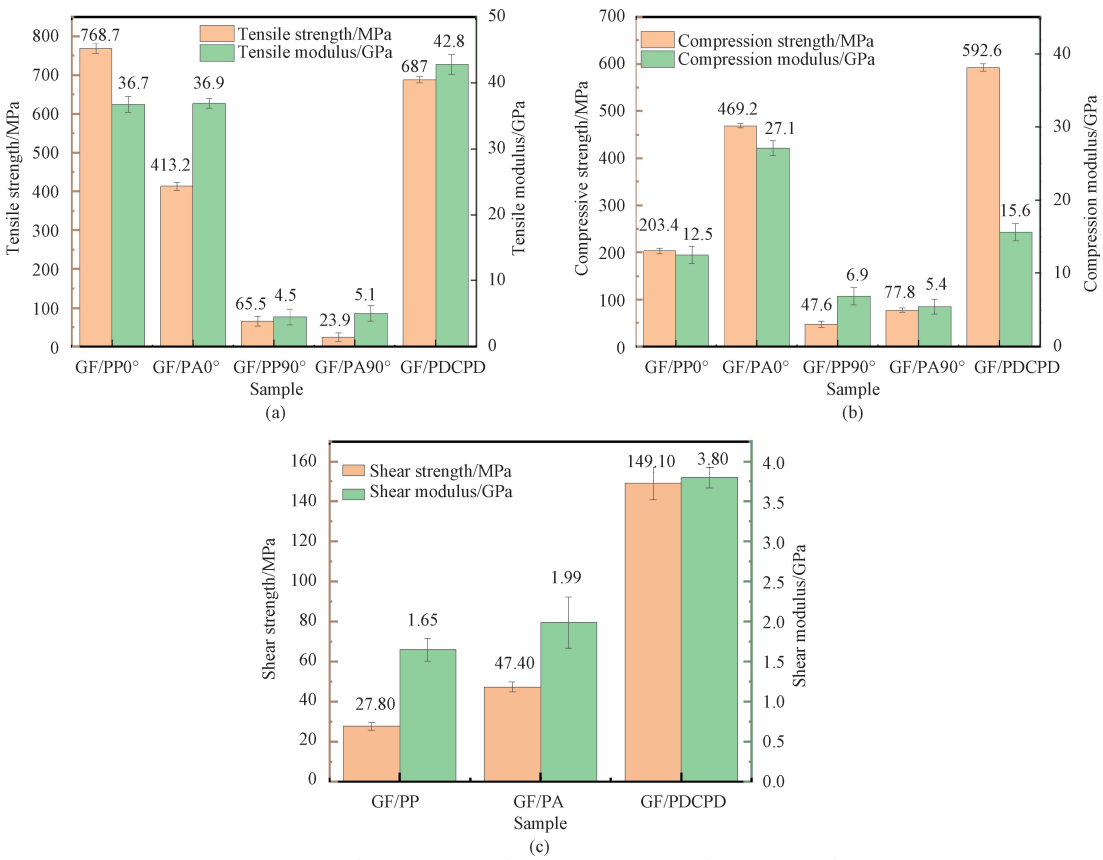

Fig. 4 Mechanical property testing results: (a) tensile test; (b) compression test; (c) shear test (0° and 90° represent the alignment of GFs along the length and width directions of the composite laminate, respectively)

The simulation analysis mainly includes the optimal ply thickness of the composite plates, the mechanical response, the final intrusion amount and the failure mode of the laminate during the impact process. Table 3 shows the Chang-Chang failure criterion parameters[32]. Among them, DFAILT, DFAILC and DFAILM control the failure strains in different directions; SOFT manages the strength reduction at the impact front to ensure model stability; FBRT and YCFAC adjust the residual fiber strength after matrix failure.

Table 3 Chang-Chang failure criterion parameters

Parameter	DFAILT	DFAILC	DFAILM	SOFT	FBRT	YCFAC
Value	0.2	−2.0	0.23	0.5	0.5	1.2

1.2.2 Comparison of impact performance of GF/PDCPD, GF/PP and GF/PA composite laminates

The impact test of composite laminates was conducted using the INSTRON CEAST 9350 impact testing device (Instron, USA), which featured a data acquisition rate of 2 MHz and a sampling frequency of 65 536 points per channel. The device utilizes a piezoelectric force sensor and boasts a 14-bit resolution for precise data collection. For the impact test, the device's software program was configured to set the impact velocity at 5 m/s and the impact energy at 120 J, as specified by the user. The test parameters including force, displacement and energy were selected for export as result parameters. To analyze defects in the composite laminates, the ultrasonic C-scanner (Tianjin Sina Intelligent Technology Co., Ltd., China) was employed. This method facilitated a comparison of simulated failure modes and enabled error analysis. By comparing the simulated and actual impact performance, the predictability of the simulation on the impact performance of composite laminates was validated. Furthermore, the impact performance of the thermosetting composite laminate GF/PDCPD was compared and analyzed against thermoplastic composite laminates GF/PP and GF/PA.

2 Results and Discussion

2.1 Optimal ply and thickness design

In order to ascertain the optimal thickness for the protective plate, impact simulations were conducted on varying thicknesses of GF/PDCPD composite laminate and thermoplastic composite laminates. Figure 5 illustrates the displacement within the shield plate at 2 mm intervals following a collision. It was observed that as the thickness of the laminate increased, the displacement decreased significantly. Notably, with increasing thickness, the primary post-crash deformation tended to occur in close proximity to the impact point and was less likely to propagate throughout the rest of the protective plate. This localized deformation pattern is advantageous for battery protection, as it indicates that the impact energy is absorbed and dissipated more efficiently in the immediate vicinity of the impact, thereby minimizing the transmission of destructive forces to other areas of the protective plate.

In order to gain a more detailed understanding of the deformation behavior, displacement along the centerline was analyzed. Figure 5(a) shows the displacement relative to the thickness of the GF/PDCPD composite laminate. It was observed that at a thickness of 2.7 mm, the displacement due to the collision was approximately 9.7 mm or higher. This indicates that the battery was not adequately protected, as the gap between the protective plate and the battery was designed to be 8.8 mm. Conversely, at a thickness of 3.0 mm, the deformation was found to be 6.8 mm or less, which was lower than the gap between the battery and the protective plate. Based on this analysis, the thickness of the GF/PDCPD composite laminates was selected as 3.0 mm for optimal impact resistance and damage mitigation. This result highlights the importance of carefully selecting the appropriate thickness for protective plates in applications such as battery protection, where structural integrity is critical for safe and reliable operation. By leveraging advanced simulation and analysis techniques, engineers and designers can develop the optimal solutions to enhance the impact resistance and mitigate the damage, thereby improving the overall safety and reliability of critical components and systems. For comparison and analysis, thermoplastic composites with the same thickness need to be prepared, and then the protective materials with good impact resistance are selected for comparative analysis.

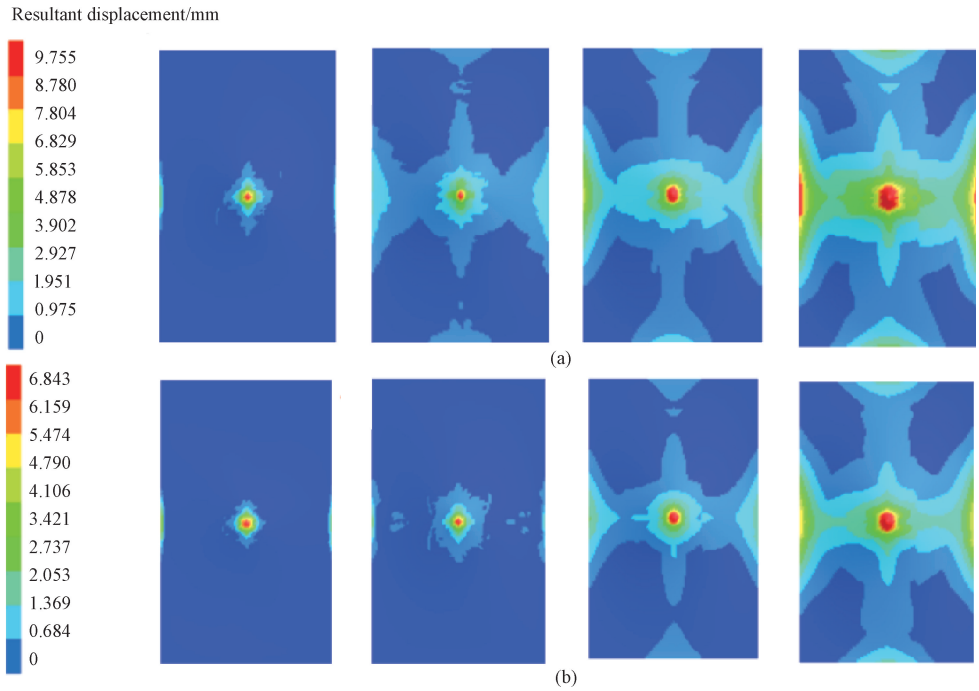

Fig. 5 Displacement relative to PDCPD composite laminate thickness: (a) 2.7 mm; (b) 3.0 mm

2.2 Comparative analysis of the shock response process

Figure 6(a) presents a comparative analysis of the mechanical response of the composites GF/PP, GF/PA and GF/PDCPD during the impact process. The displacement-load diagram illustrates the behavior of the composites under the same size and impact conditions. In the elastic stage, the peak load exhibited by GF/PDCPD (18.9 kN) surpasses that of thermoplastic composites (16.6 kN for GF/PP and 15.5 kN for GF/PA). This indicates that GF/PDCPD possesses higher strength and can withstand larger load compared to GF/PP and GF/PA. As the composite materials approach their respective peak loads, they begin to experience failure, leading to a state of significant load oscillation. In the case of GF/PP and GF/PA, the elastic potential energy stored in the flexural deformation is converted into kinetic energy as the drop weight descends. Consequently, the drop weight rebounds. Conversely, GF/PDCPD, characterized by high ductility and plasticity, does not exhibit the rebound behavior. Instead, they absorb impact energy through plastic deformation during the impact process.

This comparison highlights the distinct mechanical responses of thermoplastic composites (GF/PP and GF/PA) and GF/PDCPD, with GF/PDCPD demonstrating superior energy absorption capabilities due to its plastic deformation characteristics.

The main load drop is expected to be attributed to the onset of delamination, and the sudden occurrence of delamination leads to a sudden decrease in stiffness. Due to the high toughness of the PDCPD matrix, GF/PDCPD shows higher peak loads (18 kN) than thermoplastic composites (16.6 kN for GF/PP and 15.5 kN for GF/PA), followed by smaller stiffness losses, resulting in increased contact forces and reduced displacements. As a result, GF/PDCPD absorb more energy than thermoplastic composites (12.5% more than GF/PP and 18.0% more than GF/PA), indicating lower levels of damage and integrity loss.

Figures 6(c)–6(e) show the damage patterns occurring on the top surface (impact side) of the laminates. As shown in GF/PA (Fig. 6(e)), the damage is the most severe and obvious, mainly concentrated in the area where the punch is in contact with the laminate. From the positive impact front, all three produce visually barely visible impact damage (BVID), the damage area shows the shape of the impact head, and obvious hemispherical pits can be seen on the surface of the thermoplastic composite, as shown in Figs. 6(g)–6(h). On the back of the laminate impact, the overall shape of the damage area in GF/PDCPD (Fig. 6(g)) and GF/PA (Fig. 6(h)) is roughly circular for lower damage, and the damage of GF/PP (Fig. 6(f)) extends only in the width direction. GF/PA has a higher damage area than GF/PDCPD. The backside fibers of GF/PP and GF/PA are severely damaged, while those of GF/PDCPD are not significantly damaged, which is similar to the ultrasonic C-scan results (Fig. 9). This is due to two points: the high toughness of PDCPD and the good interface compatibility between PDCPD and the depulped GF. PDCPD and GF can form a good whole during the impact process and thus jointly resist the bending and tensile stresses generated during the impact process.

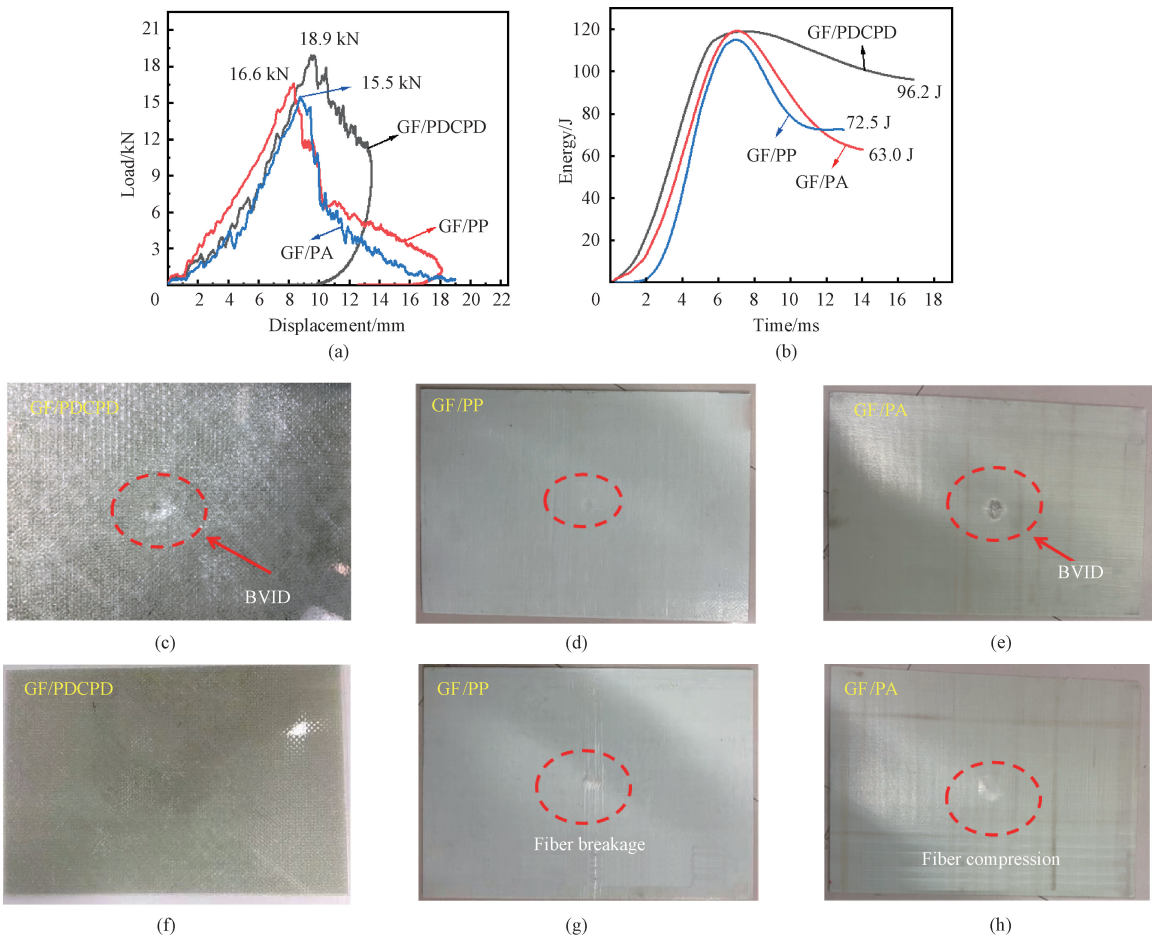

Fig. 6 Impact performance of composites: (a) force-displacement curves; (b) time-energy absorption curves; (c)–(e) top surface topographies of composite laminates after impact; (f)–(h) bottom surface topographies of composite laminates after impact

2.3 Comparative analysis of invasion volume

The intrusion of the punch during the impact process is one of the important indicators to evaluate the impact resistance of the lower bottom shield of the car because the distance between the battery and the lower bottom plate is only approximately 8.8 mm, and it is necessary to ensure that the battery structure cannot be damaged when encountering the collision of unknown objects.

Under the same impact conditions, the invasion of GF/PDCPD is the smallest (6.9 mm), which is reduced by 13.8% and 21.6% compared with that of GF/PP and GF/PA, respectively. A decrease in displacement for thermoplastic composites is observed in the *A* and *B* regions in Figs. 7(a)–7(b), which is due to the better elasticity of the composites that allows them to convert kinetic energy into elastic potential energy during the impact process. This conversion temporarily reduces the displacement as the material resists the punch, and then the displacement increases again as the punch continues to penetrate. It can be seen that the displacement of GF/PDCPD changes more slowly with time because the high toughness of GF/PDCPD during impact shows less deformation than thermoplastic composites.

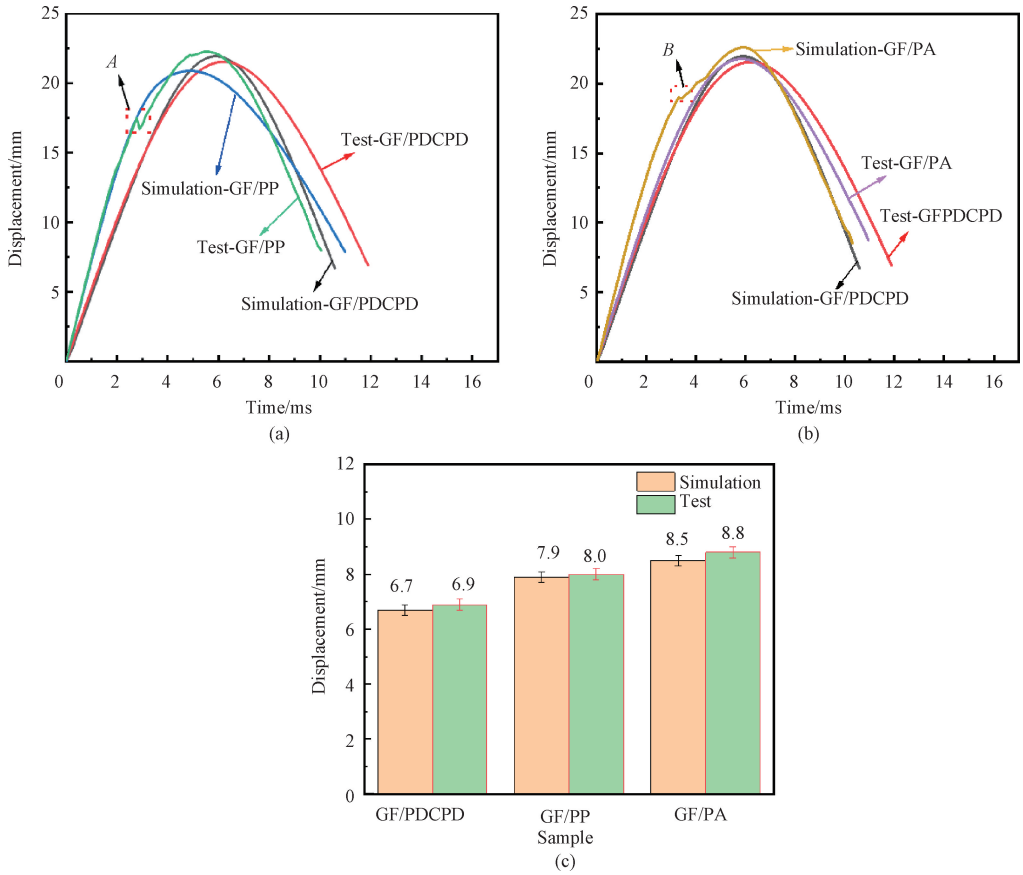

Fig. 7 Displacement-time curves of composite laminates: (a) GF/PDCPD and GF/PP; (b) GF/PDCPD and GF/PA; (c) displacement change comparison

2.4 Comparative analysis of failure modes

During the impact of composite materials, the following four failure modes can occur: both lower tension and fiber shear lead to fiber breakage; fiber compression causes fiber compression to deform or break; interfacial failure leads to separation or peeling between the matrix and the fiber; matrix failure leads to plastic deformation or rupture of the substrate.

Figure 8 shows the stress distribution cloud of the GF/PDCPD composite laminate during the impact process, and it can be seen from the simulation results that the material experiences compression failure, which leads to the compression deformation of the fiber in the process of punching. During the entire impact process of GF/PDCPD composite laminate, the stress in the length and width directions increased, and at 5.0 ms, the stress in the length and width directions was 0.649 8 MPa and 0.649 2 MPa, respectively. Due to the long path in the length direction, more stresses can be distributed in the continuous expansion of the stress along the fiber direction. Thus, the damage is not obvious, the stress in the width direction gradually increases to greater than the stress in the length direction, and the damage is more obvious.

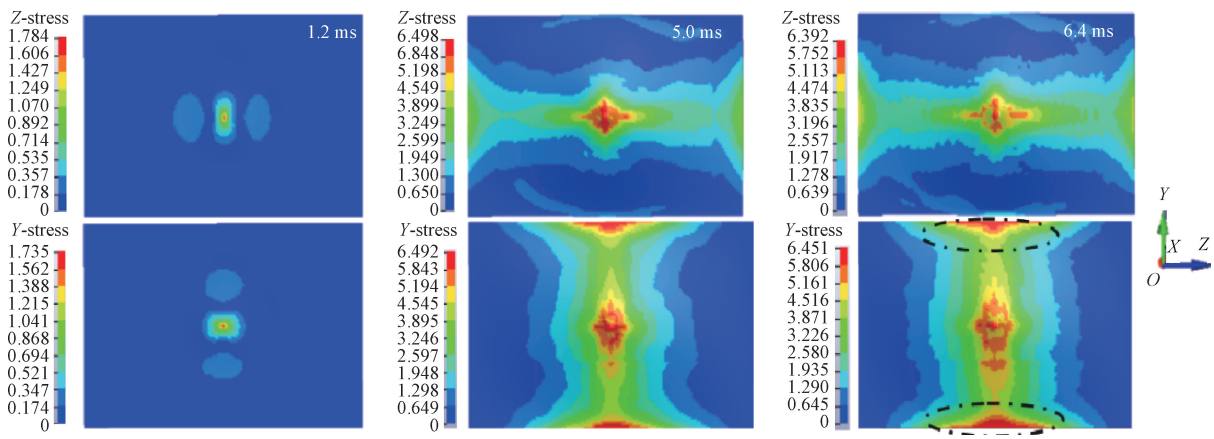

Fig. 8 Nephogram of stress distribution during impact of GF/PDCPD composite laminates

The ultrasonic C-scanner was employed to detect defects and cracks within the materials, and its findings were compared with the simulation results to validate the accuracy of the failure mode prediction in the laminate simulation model. This comparison can be seen in Fig. 9. The ultrasound C-scan results revealed that the rear side of the specimen experienced damage and failure after impact. Under the influence of the impact force, the laminate continuously bent and fractured. As the punch continued to exert pressure, peeling occurred initially on the top surface of the impact, resulting in peeling stresses and evident pits. Notably, significant damage areas were detected on the outer regions of these pits, with delamination damage extending towards the impact area. The impact process of composite laminates involved a transverse shear failure mode. During the initiation stage, numerous short interlaminar were cracked and the cracks propagated within the longitudinal layer. Once the tensile strength of the material was surpassed, interlaminar fracture occurred. Ultimately, energy was absorbed through the fracture of the laminate stack and the propagation of cracks within the layers. The sudden occurrence of delamination can lead to a reduction in material stiffness. However, due to the high toughness of the PDCPD matrix, GF/PDCPD exhibited a smaller damage area compared to other materials.

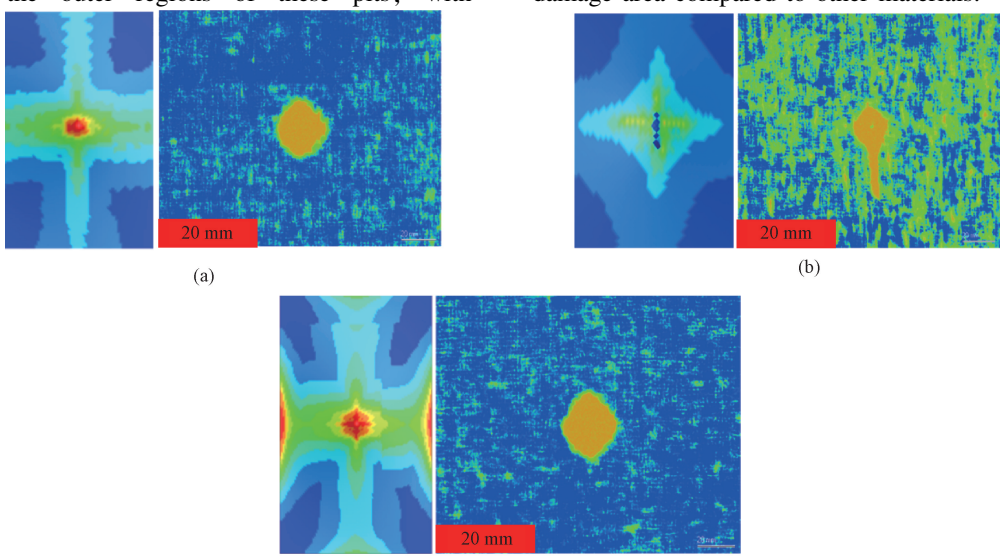

Fig. 9 Comparison of simulated failure nephogram (left) and ultrasonic C-scan (right) results of laminates after impact: (a) GF/PDCPD; (b) GF/PP; (c) GF/PA

Moreover, from the simulation results, it can be seen that the surfaces of GF/PDCPD and the thermoplastic composites (GF/PP and GF/PA) have obvious cross-shaped failure along the direction of fiber weaving. The difference is that the crack growth path of PDCPD is shorter than that of thermoplastic resin, which indicates that the high toughness of PDCPD can effectively inhibit the continuous expansion of cracks.

From the experimental and simulation results, it can be seen that the failure mode of the numerical simulation of composite laminates is similar to that of the experiment, the trend is the same, and the failure form is also the same. This shows that it is feasible to simulate the failure behavior of composite laminates during impact using the MAT54 material card in LS-DYNA. Combined with the simulation and experimental results, the impact resistance of the GF/PDCPD thermosetting composite laminates is better than that of the GF/PP and GF/PA thermoplastic composite laminates.

3 Conclusions

This paper presents a comprehensive study on GF/PDCPD, GF/PP and GF/PA composite laminates, utilizing tensile, compression and in-plane shear test data as material card parameters. An impact model for composite laminates was developed based on this data, and simulations were conducted to determine the optimal ply thickness of the composites. The study compared and analyzed the failure modes, mechanical responses, and final intrusion amounts of GF/PDCPD and thermoplastic composites (GF/PP and GF/PA). The results showed that when the thickness of GF/PDCPD was 2.7 mm, the displacement change of the laminate exceeded the maximum allowable value of 8.8 mm. However, with a thickness of 3.0 mm, the displacement change was within the target value. The comparison of failure modes indicated that thermoplastic composites experienced fiber fracture failure, while GF/PDCPD mainly exhibited matrix bending in-plane on failure with a smaller damage area. Additionally, GF/PDCPD demonstrated ductile fracture behavior with continued load-carrying capacity post-peak load, showing resistance to bottom fiber cracking and internal delamination due to their high toughness. Comparative analysis revealed that GF/PDCPD exhibited the smallest displacement changes and

the best impact resistance among the materials studied. The consistency between experimental and simulation results validated the accuracy of the simulation model in predicting failure modes and mechanical responses. This study contributes insights into optimizing composite design for enhanced impact performance and durability.

References

[1] TANG Y, YUAN W, PAN M Q, et al. Experimental investigation on the dynamic performance of a hybrid PEM fuel cell/battery system for lightweight electric vehicle application [J]. *Applied Energy*, 2011, 88(1): 68-76.

[2] XIONG H Y, TAN Z R, ZHANG R H, et al. Numerical calculation model performance analysis for aluminum alloy mortise-and-tenon structural joints used in electric vehicles [J]. *Composites Part B: Engineering*, 2019, 161: 77-86.

[3] FRAGASSA C, PAVLOVIC A, MINAK G. On the structural behaviour of a CFRP safety cage in a solar powered electric vehicle [J]. *Composite Structures*, 2020, 252: 112698.

[4] ZHAO Y, PATEL Y, HUNT I A, et al. Preventing lithium ion battery failure during high temperatures by externally applied compression [J]. *Journal of Energy Storage*, 2017, 13: 296-303.

[5] WANG Q S, PING P, ZHAO X J, et al. Thermal runaway caused fire and explosion of lithium ion battery [J]. *Journal of Power Sources*, 2012, 208: 210-224.

[6] SHUI L, CHEN F Y, GARG A, et al. Design optimization of battery pack enclosure for electric vehicle [J]. *Structural and Multidisciplinary Optimization*, 2018, 58(1): 331-347.

[7] WANG P, YANG L, GAO S, et al. Enhanced dielectric properties of high glass transition temperature PDCPD/CNT composites by frontal ring-opening metathesis polymerization [J]. *Advanced Composites and Hybrid Materials*, 2021, 4(3): 639-646.

[8] OSMAN A, ELHAKEEM A, KAYTBAY S, et al. A comprehensive review on the thermal, electrical, and mechanical properties of graphene-based multi-functional epoxy composites [J]. *Advanced Composites and Hybrid Materials*, 2022, 5(2): 547-605.

[9] CENTELLAS P J, YOURDKHANI M, VYAS S, et al. Rapid multiple-front polymerization of fiber-reinforced polymer composites [J]. *Composites Part A: Applied Science and Manufacturing*, 2022, 158: 106931.

[10] UM H J, HWANG Y T, BAE I J, et al. Design and manufacture of thermoplastic carbon fiber/polyethylene terephthalate composites underbody shield to protect the lithium-ion batteries for electric mobility from ground impact [J]. *Composites Part B: Engineering*, 2022, 238: 109892.

[11] WARD I M, HINE P J. The science and technology of hot compaction [J]. *Polymer*, 2004, 45(5): 1413-1427.

[12] AKBOLAT M Ç, KATNAM K B, SOUTIS C, et al. On mode-I and mode-II interlaminar crack migration and R-curves in carbon/epoxy laminates with hybrid toughening *via* core-shell rubber particles and thermoplastic micro-fibre veils [J]. *Composites Part B: Engineering*, 2022, 238: 109900.

[13] VALLONS K A M, DROZDZAK R, CHARRET M, et al. Assessment of the mechanical behaviour of glass fibre composites with a tough polydicyclopentadiene (PDCPD) matrix [J]. *Composites Part A: Applied Science and Manufacturing*, 2015, 78: 191-200.

[14] HU Y H, LANG A W, LI X C, et al. Hygrothermal aging effects on fatigue of glass fiber/polydicyclopentadiene composites [J]. *Polymer Degradation and Stability*, 2014, 110: 464-472.

[15] WU Z Q, LIU Q X, ZHANG H C, et al. Application of modified plastics in automobile under light weight background [J]. *Engineering Plastics Application*, 2023, 51(3): 152-156. (in Chinese)

[16] XU Y T, ZUO H F, LU X H, et al. Numerical analysis and tests for low-velocity impact damage evaluation of composite material [J]. *Journal of Vibration and Shock*, 2019, 38(3): 149-155. (in Chinese)

[17] FORMISANO A, PAPA I, LOPRESTO V, et al. Influence of the manufacturing technology on impact and flexural properties of GF/PP commingled twill fabric laminates [J]. *Journal of Materials Processing Technology*, 2019, 274: 116275.

[18] AMITH KUMAR S J, AJITH KUMAR S J. Low-velocity impact damage and energy absorption characteristics of stiffened syntactic foam core sandwich composites [J]. *Construction and Building Materials*, 2020, 246: 118412.

[19] HEIMBS S, HELLER S, MIDDENDORF P, et al. Low velocity impact on CFRP plates with compressive preload: test and modelling [J]. *International Journal of Impact Engineering*, 2009, 36(10/11): 1182-1193.

[20] GE X X, ZHANG P, ZHAO F, et al. Experimental and numerical investigations on the dynamic response of woven carbon fiber reinforced thick composite laminates under low-velocity impact [J]. *Composite Structures*, 2022, 279: 114792.

[21] PUCK A, SCHURMANN H. A comparison of numerical simulation and experimental impact behaviour of composite structures [J]. *Composite Structures*, 2014, 63(2): 173-182.

[22] IMIELIŃSKA K, CASTAINGS M, WOJTYRA

R, et al. Air-coupled ultrasonic C-scan technique in impact response testing of carbon fibre and hybrid: glass, carbon and Kevlar/epoxy composites[J]. *Journal of Materials Processing Technology*, 2004, 157/158: 513-522.
[23] ZHANG A Y, LI D H, ZHANG D X, et al. Qualitative separation of the effect of voids on the static mechanical properties of hygrothermally conditioned carbon/epoxy composites [J]. *Express Polymer Letters*, 2011, 5(8): 708-716.
[24] JANDEJSEK I, JAKUBEK J, JAKUBEK M, et al. X-ray inspection of composite materials for aircraft structures using detectors of Medipix type [J]. *Journal of Instrumentation*, 2014, 9(5): C05062.
[25] BOGENFELD R, KREIKEMEIER J, WILLE T. Review and benchmark study on the analysis of low-velocity impact on composite laminates[J]. *Engineering Failure Analysis*, 2018, 86: 72-99.
[26] JOO G, KIM J, JEONG M, et al. A practical axial crush simulation of glass-fiber MAT/PA6 composite tubes for application of an energy absorber in automobiles [J]. *International Journal of Automotive Technology*, 2021, 22(5): 1201-1213.
[27] LIU R T, LIN J P, TIAN H B. Analysis method of composite material structure's crashworthiness based on structural elements [J]. *Journal of Tongji University*, 2005, 33(3): 366-371. (in Chinese)
[28] CHENG C, ZHANG C Y, CHEN Z G, et al. Polydicyclopentadiene toughened epoxy resin and its carbon fiber composites via sequential polymerization[J]. *Polymer Composites*, 2023, 44(10): 6929-6943.
[29] OBANDE W, MAMALIS D, RAY D, et al. Mechanical and thermomechanical characterisation of vacuum-infused thermoplastic- and thermoset-based composites[J]. *Materials & Design*, 2019, 175: 107828.
[30] ZIAEE M, NASERI I, JOHNSON J W, et al. Frontal polymerization and three-dimensional printing of thermoset polymers with tunable thermomechanical properties [J]. *ACS Applied Polymer Materials*, 2023, 5(3): 1715-1724.
[31] YOO H M, JEON J H, LI M X, et al. Analysis of curing behavior of endo-dicyclopentadiene using different amounts of decelerator solution [J]. *Composites Part B: Engineering*, 2019, 161: 439-454.
[32] SHAO J R, LIU N, ZHENG Z J. Numerical comparison between Hashin and Chang-Chang failure criteria in terms of inter-laminar damage behavior of laminated composite[J]. *Materials Research Express*, 2021, 8(8): 085602.

GF/PDCPD 热固性复合材料汽车底护板的冲击行为及失效模式研究

梅忠浩[1], 裴志磊[1], 程乐乐[1], 闵 伟[1], 高睿泽[1], 程 超[1,2], 周 飞[3], 余木火[1], 孙泽玉[1*]

1. 东华大学 材料科学与工程学院, 上海轻质结构复合材料重点实验室, 上海高性能纤维与复合材料协同创新中心, 上海 201620
2. 上海碳纤维复合材料创新研究院有限公司, 上海 201512
3. 中石化上海石化有限公司, 上海 200540

摘 要: 基于 LS-DYNA (由 Livermore 软件技术公司开发的有限元分析软件) 建立了玻璃纤维 (glass fiber, GF) /聚双环戊二烯 (polydicyclopentadiene, PDCPD) 复合材料的冲击模拟模型, 确定了其最佳厚度为 3.0 mm。最终的侵入深度可控制在 8.8 mm 以内, 符合电池电动汽车保护材料的性能标准。对 GF/PDCPD、GF/聚丙烯 (polypropylene, PP)、GF/聚酰胺 (polyamide, PA) 复合材料在冲击过程中失败模式的比较分析表明, GF/PDCPD 表现出压缩失效模式和韧性断裂, 导致损伤区域较小。相比之下, GF/PP 和 GF/PA 则表现出纤维断裂失效, 导致更大的损伤区域。研究探讨了 GF/PDCPD 的成型过程和抗冲击性能。GF/PDCPD 抗冲击性能优于 GF/PP 和 GF/PA, 更符合电池电动汽车保护材料的性能标准。LS-DYNA 模拟的可预测性和准确性得到了验证, 为进一步深入研究提供了理论基础。

关键词: 热固性复合材料; PDCPD; GF/PP; GF/PA; LS-DYNA 仿真; 冲击性能; MAT54